Segmental Orientation Behavior of Flexible Water-Blown Polyurethane Foams

J. C. MORELAND and G. L. WILKES*

Department of Chemical Engineering and Polymer Materials & Interfaces Laboratory, Virginia Polytechnic Institute and State University, Blacksburg, Virginia 24061-6496

ROBERT B. TURNER

Urethanes, Polymers & Product Research, Dow Chemical Company, Freeport, Texas 77541

SYNOPSIS

The ambient temperature structure–property orientation behavior in two different polyurea–urethane polymers (one cross-linked and one linear) was measured by using infrared dichroism along with mechanical response. Thin films (plaques) thermally compression-molded from TDI-polypropylene (PO) flexible water-blown polyurea–urethane foams and solution-cast TDI–PO polyurea–urethane elastomers were studied. Segmental orientation was measured as a function of elongation and relaxation, as well as of hysteresis behavior. The level of strain was 50–70% for the plaques and up to 240% for the elastomer. The soft segments for both materials exhibited a low state of orientation with elongation. Small changes in orientation with time and upon cyclic straining were also observed for the soft segments. Significant transverse orientation upon stretching was observed in the hard segments of the plaques and up to elongations of 100% for the elastomer. The transverse behavior of the hard segments in the plaques pressed from the foams was attributed to both the smaller hard domains as well as to the polyurea aggregates that have been reported to be present in flexible foams. This transverse behavior also suggested that the smaller hard domains and the polyurea aggregates possess a lamellarlike structure. At low strain levels (up to 50%), only small amounts of orientation hysteresis as well as mechanical hysteresis were observed for the hard segments of the plaques as well as for the elastomer. No significant relaxation in orientation was detected for the hard segments of both materials at a 30% strain level.

INTRODUCTION

Structure–property relationships in polymers are evaluated to obtain a better understanding of the resulting morphology and its relationship to the mechanical and related properties. The majority of the reports in the literature on these relationships in polyurethanes has concentrated on the thermoplastic elastomers made from urethane chemistry.[1-10] However, even though flexible foams make up 50% or more of the polyurethanes manufactured, there have been very few reports on the structure–property behavior in these important materials. With this in mind, such a study of the *solid portion* of flexible water-blown polyurethane foams was undertaken. In the first report from this study, the morphology of the solid portion of these foams was evaluated by using several different structural techniques.[11] An overview of these earlier results are necessary before proceeding with the newer approach discussed in this paper, which addresses two of these same foam materials.

* To whom correspondence should be addressed.

Journal of Applied Polymer Science, Vol. 43, 801–815 (1991)
 CCC 0021-8995/91/040801-15$04.00

In the previous study, a systematic series of four slabstock foams that varied in hard segment content (21–34 wt %) were characterized by using several different structural techniques.[11,12] Furthermore, the thermal compression-molded plaques of these foams were also studied in order to analyze the material composing the foam *independent of its cellular geometry*. Two of the structural techniques, small angle X-ray scattering (SAXS) and dynamic mechanical spectroscopy (DMS), gave evidence that a two-phase morphology that is somewhat similar to that of urethane and urea–urethane elastomers exists in the foams as well as in the corresponding molded plaques. The DMS results exhibited a rubbery plateau and a fairly sharp soft segment glass transition that was rather independent of hard segment content. The SAXS results detected scattering centers (hard domains) that were approximately 7 nm apart and possessed fairly sharp phase boundaries. Both of these techniques noted somewhat better phase separation in the plaques, which was possibly induced by the compression-molding process. Transmission electron microscopy (TEM) results showed evidence of what were considered to be large urea-based aggregates that increased in size from approximately 100–400 nm with increasing hard segment content in both the foams and their respective plaques. The urea-based aggregates were suggested to be due to the precipitated urea phase that has been reported by other workers using FTIR to study the foaming process.[13–15] The wide angle X-ray scattering (WAXS) patterns of the foams—particularly those of higher hard segment content—suggested that some hard segment order exists due to the possibility of hydrogen bonding between the hard segments. The WAXS patterns did not appear to change significantly upon compression molding, thus indicating the thermal process did not have a major effect on the hard segment order.

In summary of the structural studies for the solid portion of the foams, the earlier authors proposed the simplified schematic morphological model shown in Figure 1.[11] The larger structures' specified "urea" represent the urea-based aggregates that were thought to be of a reinforcing nature within the system. Also represented in Figure 1 are the smaller hard domains that should not be confused with the larger aggregate structures. The smaller hard domains are believed to be rather typical in size of those that exist in urea–urethane and urethane elastomers of comparable hard segment content. An important difference, however, from that of the elastomers is the presence of a covalent network in the foam. This, of course, influences the long-term creep, stress relaxation, and level of extensibility.[11]

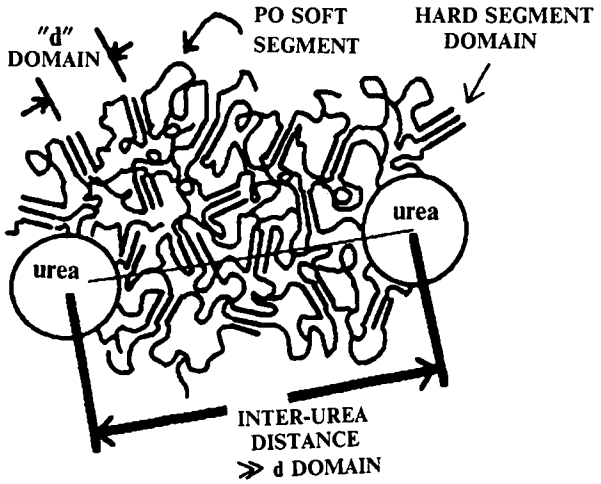

Figure 1 Initial morphological model for the solid portion of flexible water-blown foam. The "*d*" domain is approximately 7 nm, and the size of the urea aggregates range from 100 to 400 nm with increasing hard segment content. The "sticklike" hard segments are not necessarily as linear or as uniform in length as the figure implies. The actual size of the urea aggregates is larger than they appear in the model (taken from Ref. 11).

With this first approximation morphological model, a better understanding of the structure–property behavior in the solid-state portion of flexible foams was partially obtained. In making this understanding more complete, a relationship between the viscoelastic properties of flexible foams such as compression set and fatigue and the morphological features needs to be developed. One approach to obtaining a better understanding of this relationship is to measure the respective orientation behavior of the hard and soft segments in the plaques of the foams under uniaxial extension. This approach has been instrumental in studying the structure–property behavior in urethane and urea–urethane elastomers.[1–6] The technique often used to measure the orientation behavior in segmented polyurethane elastomers is linear IR–dichroism. This method utilizes linearly polarized radiation in characterizing the orientation behavior of specific chromophoric groups of a polymer molecule. By doing so, this technique has the ability to separate the orientation behavior of the different segments in multicomponent or multiphase materials. For example, Seymour et al. measured the orientation as a function of elongation for a segmented polyether urethane by characterizing the hard segment ori-

Table I Formulation Components for Flexible Water-Blown Foams

Isocyanate	T-80, 80 : 20 mixture of 2,4- and 2,6-isomers of toluene diisocyanate (Dow Chemical)
Polyol	Voranol 3100, a 3000 MW propylene oxide glycerine initiated polyether polyol; approximately trifunctional (Dow Chemical)
Water/blowing agent	Deionized water—no chemical blowing agent used
Catalysts	T-9, a tin catalyst commonly known as stannous octate (MET Chemical) DABCO 33LV, an amine catalyst that is triethylenediamine in dipropylene gycol (Air Products)
Surfactant	BF-2370, a silicone surfactant (Goldschmidt)

entation utilizing the N — H group and the soft segment orientation with the CH_2 group.[1] The authors reported observing higher levels of orientation for the hard segments than for the soft segments at the same level of deformation. This was expected since the hard segments tend to retain their level of orientation upon deformation due to their rigidity, whereas the flexible soft segments tend to relax quickly and take on a more random orientation. In addition to measuring the segmental orientation induced upon deforming a thin polymer film to different levels of strain, the relaxation of the different segments in polyurethane elastomers has also been followed over time at a fixed level of deformation.[1,2] Clearly, measurement of the segmental relaxation behavior has been helpful in understanding the viscoelastic behavior.

In continuation of the structure–property study on the flexible water-blown polyurethane foams by Armistead et al.[11] the orientation behavior of the compression-molded plaques of two of the four foams has been evaluated by using IR–dichroism along with their mechanical response. The results of the segmental orientation behavior are given as a function of elongation and time as well as of cyclic deformation. Furthermore, comparisons of these data to related orientation results obtained for a TPU–polyurea–urethane elastomer have also been made and will be discussed.

EXPERIMENTAL

Materials and Thin Film Preparation

The two foams used in this work were the two lowest hard segment content materials of the four flexible slabstock foams used in the earlier morphological study by Armistead et al.[11] The preparation of these foam materials has been described elsewhere.[11] The formulation components used are given in Table I. The two foams used differ in that foam 1 was produced with 2 parts of water per 100 parts polyol (pph), whereas foam 2 was made with 3 pph water. In both cases, the isocyanate index was maintained at 110 while keeping the other component additions the same. This results in foam 1 having a 21 wt % hard segment content, whereas foam 2 has a slightly higher hard segment content of 26 wt % (calculation of hard segment wt % does not consider the 10% excess isocyanate). The basic repeat units for the hard and the soft segments of these foams are shown in Scheme 1.

As stated in the Introduction, the compression-molded plaques were used in the present IR–di-

(1) PPO repeat unit – soft segment

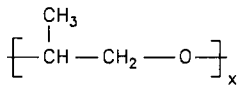

(2) Polyurea repeat unit – hard segment

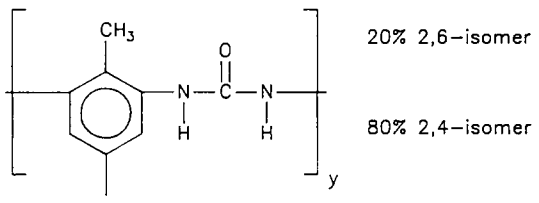

Scheme 1 Basic repeat units for PPO soft segment and polyurea hard segment based on water extended TDI-80.

chroism studies. These were made by compression molding the foams at 204°C for 10 min. In most cases, in order to obtain thin-enough plaques so that sufficient sample transmittance could be obtained, the foams were subjected to a pretreatment process before compression molding. This process consisted of first soaking (swelling) the foams in DMF overnight. By swelling the foams, it has been shown by Armistead that a small weight percentage was removed.[16] The weight percentage of material removed from foam 1 was 2% and slightly more for foam 2 (4.1%), which contains a higher hard segment content of the two foams. An additional liquid, THF, was also used to swell foams 1 and 2 since it is less likely to interact with the hard phase in comparison to that of DMF. The weight loss values obtained when using THF were lower than those obtained when using DMF as the liquid. Thus, these results suggest that the sol fraction extracted from DMF consists mostly of the hard segment phase. This speculation was supported by analyzing the extract with IR and detecting that urea-based compounds were the predominant species.[16]

After swelling the foams, the solvent was then completely removed by storing the foams in a vacuum oven at 50°C for at least 24 h. The foams were then compression-molded using the above conditions. By using the pretreatment process before compression molding, the plaques were somewhat more transparent than if the pretreatment process had not been used. Thus, it appears that thinner and more transparent plaques were obtained as a result of the partial extraction of some of the large urea-based aggregates (the hard segments of the smaller domains should clearly not display extractability). The nomenclature that will be used for the plaques is defined in Table II.

A urea–urethane thermoplastic elastomer was also used in this investigation for purposes of comparison. The urea–urethane elastomer was made from a 80:20 mixture of TDI (see Table I) and a 2000 MW polypropylene oxide diol (P2000) with methylene-bis(2-chloroaniline) (MOCA) as the chain extender. The elastomer was prepared in a two-step reaction sequence and contained 31 wt % hard segment content. For this investigation, the urea–urethane elastomer will be referred to as the "PUU" elastomer. Thin films were obtained by dissolving this elastomer in DMF and then casting this solution onto a Teflon surface. This solution was allowed to stand overnight, and then the excess solvent was removed in a vacuum oven at 50°C. The concentration of the solution was approximately 0.015 g/cc, and the resulting film thickness was in the range of 0.5–1.0 mils.

Table II Nomenclature for Compression-molded Plaques

Foam	DMF	THF	No Solvent	Plaque
1	—	—	x	1
1	—	x	—	1-THF
1	x	—	—	1-DMF
2	x	—	—	2-DMF

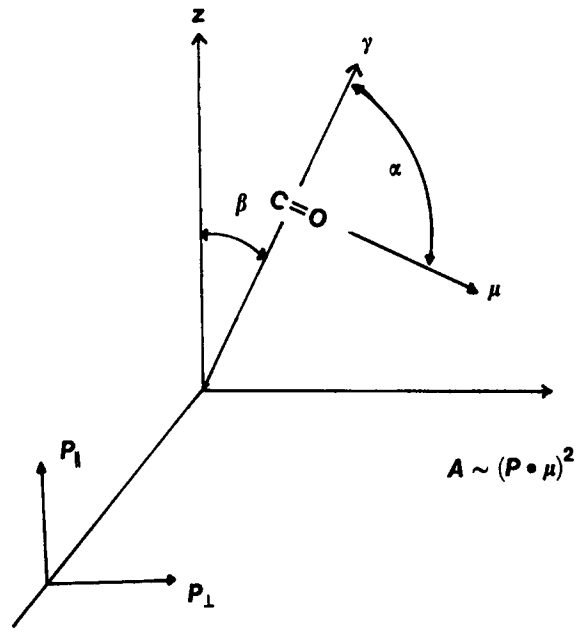

Figure 2 Coordinate system for linear dichroism: chain axis in relation to deformation axis (z is the stretch axis and μ is the transition moment).

Linear IR–Dichroism Theory

IR–dichroism provides a method to obtain the degree of orientation of polymer films. This is done by measuring the dichroic ratio, D, this ratio being defined as

$$D = \frac{A_{\parallel}}{A_{\perp}} \tag{1}$$

where $A_{\parallel}$ and $A_{\perp}$ are the absorbances of linearized polarized radiation with the polarization vector parallel and perpendicular to the deformation axis, z, respectively (see Fig. 2). The peak heights are normally utilized in measuring the absorbances.

The state of orientation can be expressed by the

Herman's orientation function, f, where f is given as

$$f = \frac{3\langle \cos^2\beta \rangle - 1}{2} \quad (2)$$

and β is defined in Figure 2 as the angle the chain axis makes with the deformation axis. In addition, f is related to D and the transition moment angle, α, by the following equation:

$$f = \left(\frac{D_0 + 2}{D_0 - 1}\right)\left(\frac{D - 1}{D + 2}\right) \quad (3)$$

where $D_0 = 2 \cot^2\alpha$ and α is defined in Figure 2 as the angle the transition moment of the selected absorbing group makes with the chain axis.[17]

The upper and lower limits of eq. (3) are defined by eq. (2) such that for parallel alignment of the chains, f equals 1 and for perpendicular alignment f equals -0.5 for D_0 equal to 0, the lower limit of eq. (3) does approach -2 as D approaches infinity, which appears to contradict the last statement. However, eq. (2) is defined for uniaxial orientation only, and, thus, the lower limit when assuming uniaxial orientation can be shown to be -0.5. However, in certain cases of biaxial orientation, it can be shown that the lower limit of the orientation function approaches minus one.[18,19]

If specific absorption bands of known α can be selected, eq. (3) provides a means to obtain the state of orientation for the specific components or phases in a material. The absorbing groups of interest for the plaques and the PUU elastomer are summarized in Table III along with their absorbing frequencies, transition moment angles, and component representation. As an example from Table III, the N—H stretching vibration is mostly representative of the hard segment and, to a smaller extent, the interface of the hard and soft phases. It has a reported transition moment angle of 90°.

Equipment

The equipment utilized to obtain the molecular orientation by IR–dichroism as well as the simultaneous mechanical response was an infrared source, a suitable polarizer, and an appropriate mechanical apparatus. A Nicolet 5DXB FTIR spectrometer with 4 cm^{-1} resolution was used as the infrared source. An IR–grid polarizer with KRS-5 substrate material with 70% maximum efficiency was used to polarize the infrared radiation parallel and perpendicular to the deformation axis. An automated stretching apparatus was constructed for the purpose of this work. The design criteria for this apparatus and a description and the operation of this apparatus are briefly given in the paragraphs to follow.

The main objective for the rheo-optical study was to *simultaneously* collect polarized FTIR data with the stress–strain properties of thin film samples. In order to do this, a mechanical apparatus was required to fit into the FTIR spectrometer sample chamber. Some of the other criteria for this apparatus were as follows: (1) deform the samples from both ends for purposes of maintaining a constant "sample zone" for impingement by the incident beam, (2) allow for variability of strain rate and level of elongation, (3) simultaneously monitor stress and strain behavior of polymer samples by an on-line computer during the orientation measurements, and (4) control temperature in the range of 20–150°C with a thermal chamber. Many of these criteria were obtained by using several of the design features of a system described by Siesler.[3]

Using the above criteria, the rheo-optical me-

Table III Absorbing Frequencies for Plaques and the PUU Elastomer

Frequency (cm^{-1})	Assignment[a]	Transition Moment Angle (°)[b]	Segmental Representation
3300	ν(N—H)	90	Hard segment, interface
2940	$\nu(CH_2)$	90	Soft segment
2860	$\nu(CH_2)$	90	Soft segment
1730	$\nu(C{=}O)_f$	78	Interface
1640	$\nu(C{=}O)_{ur}$	78	Hard segment
1475	$\delta(CH_2)$	90	Soft segment
1370	$\omega(CH_2)$	0	Soft segment

[a] ν = stretching vibration, ω = wagging mode, δ = bending mode.
[b] Taken from Refs. 4 and 6.

chanical apparatus was constructed, and a close-up photograph is shown in Figure 3(a) of this apparatus with the polarizer. The different components in Figure 3(a) are the linear motors (1), a load cell (2), an amplifier (3), a grid polarizer (4), an arm used to rotate the polarizer (5), and a thin film sample (6). The linear motors separate simultaneously and therefore *stretch the sample from both ends*. The movement of the linear motors is controlled by inputting a simple Basic computer command that specifies the velocity of travel, i.e., crosshead(s) speed and the travel distance that determines the strain or elongation. The travel of the linear motors is very smooth even when applying a force on the motors. Upon stretching the thin film sample, the force that is exerted is detected electrically and amplified by the load cell [see Fig. 3a (2)]. This signal is then digitized by an analog-to-digital converter and stored in the computer.

The mechanical apparatus is shown in Figure 3(b) inside of the FTIR spectrometer sample chamber. The maximum sample extension inside the chamber is 250% for an initial clamp-to-clamp separation distance of 25 mm. One of the other features of the stretching apparatus, but not shown here, is the addition of a thermal chamber that can operate from ambient to 150°C.

Deformation–IR Dichroism Experiments

In utilizing the above rheo-optical system, three different types of deformation experiments were performed at ambient conditions (approximately 25°C and 20–30% relative humidity) in obtaining the orientation behavior simultaneously with mechanical response. They were stress–strain, cyclic deformation, and stress relaxation. The stress–strain and the cyclic deformation tests involved stretching a thin film sample at an extension rate of 400%/min in 10% increments of elongation. At the end of each increment, the dichroism measurements were made after "stress equilibration" was nearly reached. This usually took 1–5 min depending on the sample and the strain level. The measurements involved taking two IR spectra (25 scans each) with the polarizer parallel and perpendicular to the stretch direction. The IR spectra for the plaques as well as for the PUU elastomer contained no band overlap in the regions of interest (see Table III). In determining the dichroic ratio for the chromophoric groups of interest, the peak heights were then measured using a peak-picker routine that was part of a Nicolet software package. Before measuring the peak heights for N—H, the spectra were smoothed due to multiple peaks in the N—H region of the IR spectrum. The smoothing routine utilizes a moving window where the width of the window is the number data points that are averaged. The number of data points or the width of the window used in the data analysis of the N—H region was 9. During the stress–strain and cyclic deformation experiments, the mechanical behavior was also monitored for each increment of strain to eventually give the "stress–strain" behavior.

The stress relaxation experiment was used to provide an indirect measure of the "general" orientation behavior with time. The test involved stepping to a 30% strain level and then making the dichroism measurements with time. Only 10 scans for each polarization direction were used, which took 30 s to obtain the measurements. The stress relaxation behavior was also obtained simultaneously.

The orientation behavior as well as the mechanical data that were obtained represent single measurements and not an average over many experimental tests. However, the experiments were repeated for all samples, and the same general behavior was reproduced. The maximum range of error in the orientation function was ±.05 orientation units. This range was determined by averaging results used to evaluate the performance of the rheo-optical system described earlier.

RESULTS AND DISCUSSION

Sample Characterization of Pretreated Plaques

As mentioned in the Experimental section, a pretreatment process was used to make thinner plaques from the foams to be used for the IR–dichroism studies. In evaluating the possible effects of this pretreatment process on the morphology of the plaques, three structural techniques, DMS, WAXS, and SAXS, were utilized. These results are represented by those obtained for plaque 2-DMF along with plaque 2 for comparison.

The WAXS patterns for plaques 2 and 2-DMF (not shown here) exhibit an apparent diffraction peak at 0.45 nm, which is slightly sharper for plaque 2. Armistead et al. have suggested that the apparent diffraction peak at 0.45 nm is an indication of increased order in the hard segments and is speculated to be caused by a paracrystalline texture of the TDI-hard segments arising from hydrogen bonding.[11] As suggested earlier by the weight loss results, the WAXS results also indicate that a small amount of the polyurea phase is removed during pretreatment

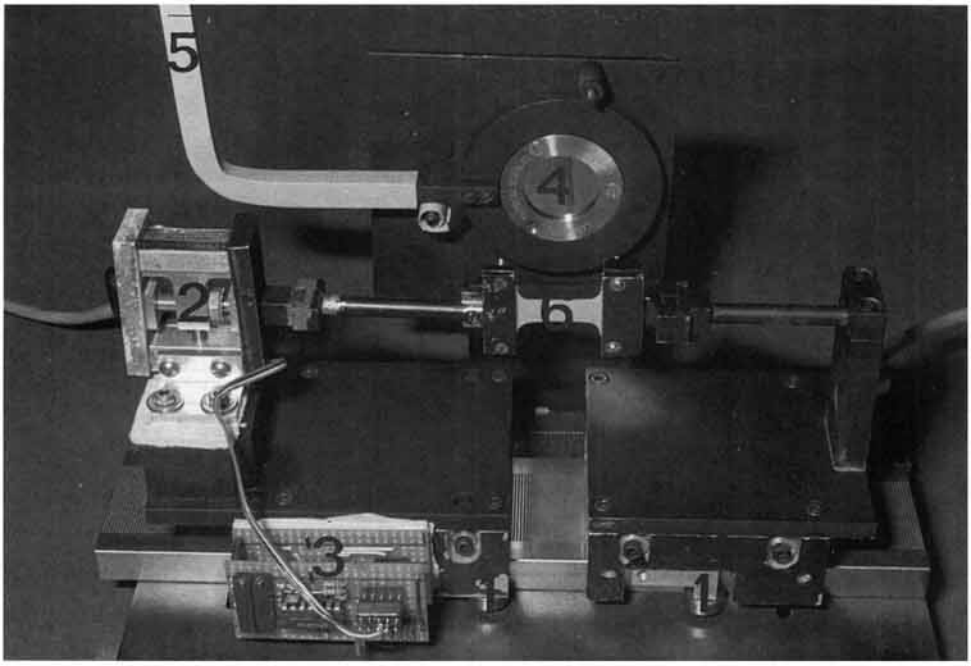

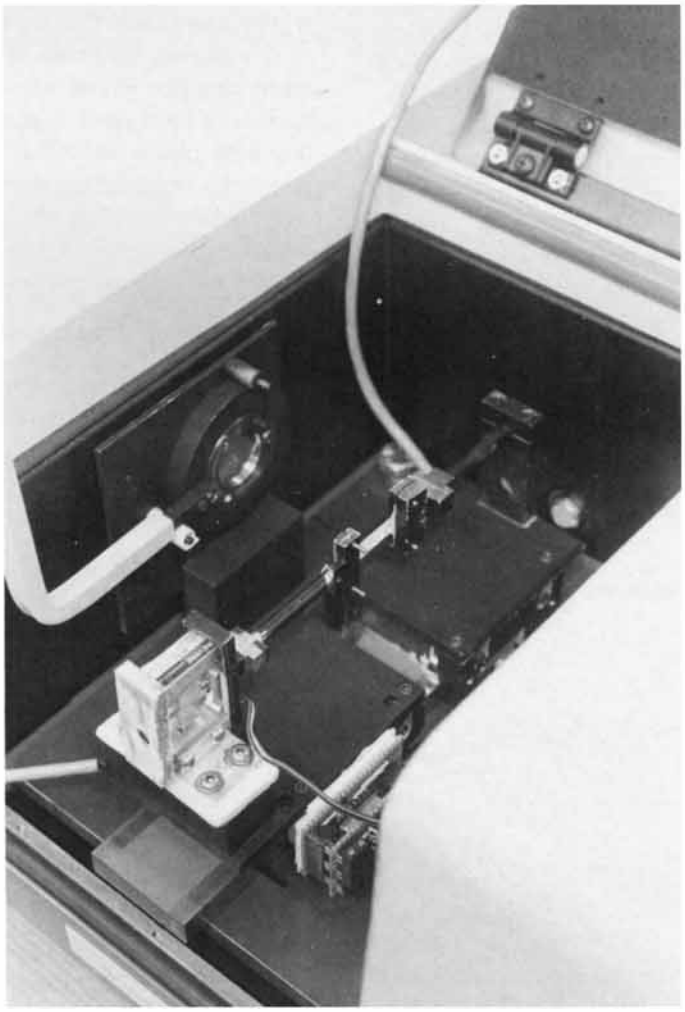

Figure 3 (a) Rheo-optical stretching apparatus: (1) linear motors, (2) load cell, (3) amplifier, (4) grid polarizer, (5) arm to rotate polarizer, and (6) sample; (b) rheo-optical stretching apparatus in FTIR sample chamber.

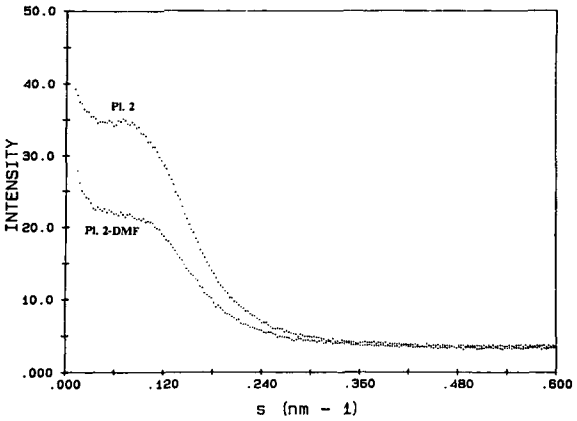

Figure 4 SAXS scattering profiles for plaques 2 and 2-DMF.

of the foams. Another lesser possibility for the changes in the WAXS behavior is that some disruption of the hydrogen bonding has taken place, leading to some loss in packing regularity.

The SAXS scattering profiles shown in Figure 4 for plaques 2 and 2-DMF also show a difference. The scattering intensity for the low-angle region was nearly 45% higher for the unextracted plaque. There are several possibilities that could give rise to this difference in scattering intensity. The most likely is that due to the fact that some of the hard-phase polyurea components are lost by extraction there is a decrease in the scattering. Another possibility is that the solvent interaction during swelling the foams caused some changes in size and shape of the smaller hard domains. However, this does not appear to have taken place since there is no major shift in the shoulder (average interdomain spacing) for the pretreated plaque (see Fig. 4).

In Figure 5, the storage modulus–temperature behavior is shown for plaques 2 and 2-DMF, for which there appears to be some differences. The most noticeable difference is that the modulus for plaque 2-DMF in the rubbery plateau region is approximately a factor of 2 lower than that of plaque 2. Furthermore, plaque 2-DMF softens at about 190°C, which is 10°C lower than the softening temperature of plaque 2. This decrease in modulus and temperature stability are also believed to be caused by the partial extraction of the polyurea precipitates (free urea-containing moieties) and/or disruption of the hydrogen bonds between the hard segments. This suggests that the urea precipitates are acting as finely dispersed filler particles to strengthen the plaque structurally.

Overall, the results from the three structural techniques reveal that there are some small changes in the morphology that are caused by the pretreatment process. These small but noticeable changes appear to be related to the partial extraction of the polyurea phase as well as to the disruption of the hydrogen-bonding network, which most likely takes place while swelling the foams in the interactive liquid.

Orientation–Elongation Behavior

The orientation–elongation behavior obtained at ambient conditions for plaque 1-DMF of foam 1 and

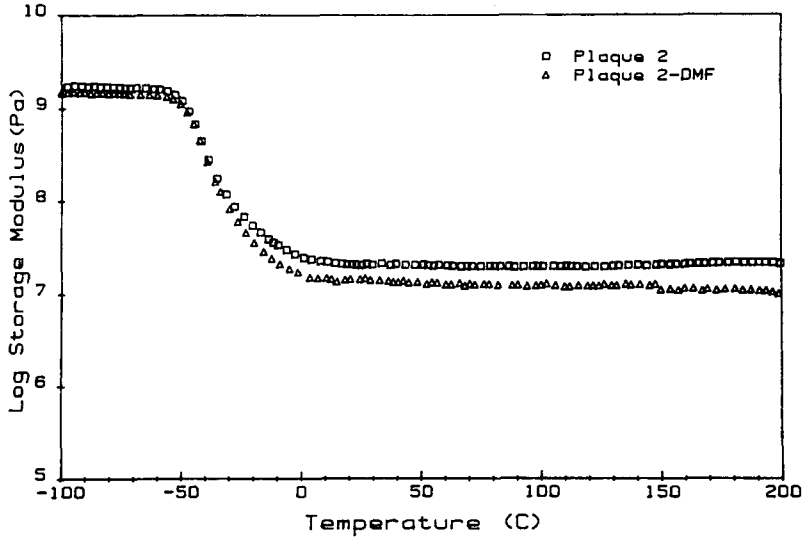

Figure 5 Storage modulus curves for plaques 2 and 2-DMF. The frequency was 11 Hz.

for plaque 2-DMF of foam 2 are shown in Figures 6 and 7, respectively. The soft segment orientation behavior that is represented by the $\delta(CH_2)$ group for plaque 2-DMF and the $\omega(CH_2)$ group for plaque 1-DMF display very little change in orientation with elongation. The orientation level with elongation at the interface of the hard and soft components is positive and slightly greater than that of the soft segments as shown by the $(C{=}O)_f$ absorbing group in Figures 6 and 7. On the other hand, the hard segments exhibit significant amounts of negative orientation with elongation shown by the $\nu(N{-}H)$ group in Figures 6 and 7 and the $(C{=}O)_{ur}$ group in Figure 7. The orientation behavior for plaques 1-DMF and 2-DMF are very similar, with the exception of the small difference in the hard segment orientation level at the higher elongations (to be addressed later). In addition, the orientation behavior of plaque 1-DMF shows the same trends and similar orientation levels to that of plaque 1 (behavior not shown here) that was *prepared without using the pretreatment process*. This result, of course, *suggests that the pretreatment process has little if any effect on the orientation behavior* in the plaques and is also rather consistent with the results discussed above from the structural techniques for plaque 2-DMF and plaque 2.

The orientation–elongation behavior for plaque 1-DMF (Fig. 6) and plaque 2-DMF (Fig. 7) compare well with the orientation–elongation behavior shown in Figure 8 for the PUU elastomer up to the range of 75% elongation. The PUU elastomer consists of only linear chains and has a microphase morphology

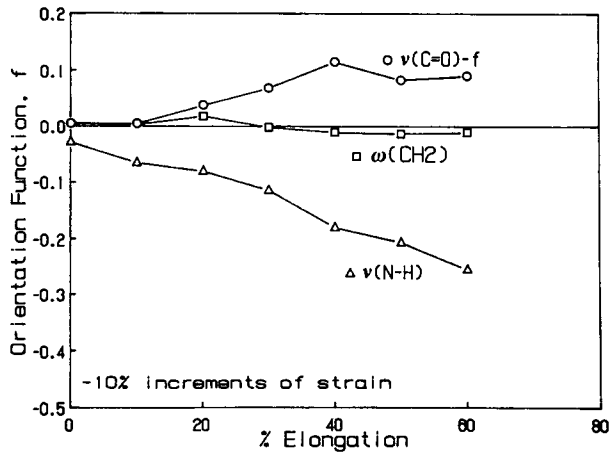

Figure 6 Orientation–elongation behavior for plaque 1-DMF. Behavior for $\nu(C{=}O)_{ur}$ not shown because of unreliable orientation behavior caused by high absorbance values.

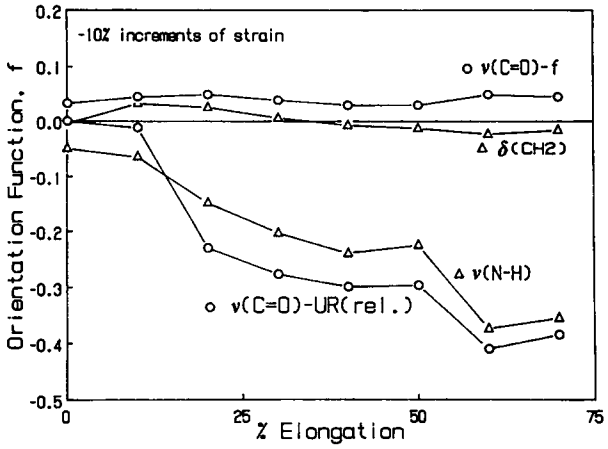

Figure 7 Orientation–elongation behavior for plaque 2-DMF. The orientation values are given as relative values for $(C{=}O)_{ur}$ due to the rather high absorbance values. Behavior for the $(C{=}O)_{ur}$ groups was reproducible.

typical of urea–urethane elastomers. The orientation behavior of the plaques and the PUU elastomer, furthermore, have the same trends reported in the literature for both diphenylmethane diisocyanate (MDI)- and TDI-based urea–urethane elastomers that utilized a polytetramethylene oxide (PTMO) soft segment.[4-6,20,21]

The low state of orientation for the soft segments of plaques 1-DMF and 2-DMF as well as for the PUU elastomer is attributed to the entropy-driven relaxation of the soft segments leading to more disorder. The soft segments in the plaques and the PUU elastomers appear to have a greater effect on the orientation at the interface in comparison to the hard segments (see Figs. 6–8). It is important to remember that the interface between the hard and

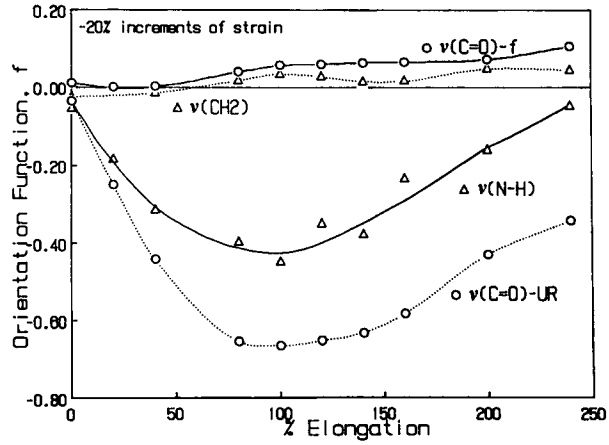

Figure 8 Orientation–elongation behavior for the PUU elastomer.

soft segments consists of two components: (1) the interfacial region that exists around the hard domains, and (2) the individual hard segments that are surrounded by the soft segment matrix. In explaining the orientation behavior at the interface for a set of MDI–PTMO urea–urethane elastomers, Wang and Cooper have suggested that the retractive force that accompanies the relaxation of the soft segments could exert a tension on the urethane linkage at the interface, therefore leading to a small amount of a positive orientation for the $(C{=}O)_f$ group (4). This may also apply to both components of the interface for the hard and soft segments in the plaques and the PUU elastomer.

The orientation level for the $\nu(C{=}O)_{ur}$ groups is, for the most part, more negative than for the $\nu(N{-}H)$ groups for plaque 2-DMF and the PUU elastomer (see Figs. 7 and 8). This is expected, since the N—H groups are present in *both* the urea and urethane linkages. As discussed above, the urethane groups exhibit positive orientation levels, which suggests that the orientation of the $\nu(N{-}H)$ groups should be higher than for the $(C{=}O)_{ur}$ groups. Several investigators of urea–urethane elastomers have also reported the same trend for the orientation–elongation behavior up to elongations of 100–200%.[4-6,20-22] In addition, these investigators along with those that have studied segmental urethane elastomers have suggested similar explanations for the negative orientation of the hard segments.[1-6,21] For the most part, these investigators suggested that the negative orientation or transverse orientation at the smaller elongations (< 200%) can be attributed to the hard domains possessing lamellarlike textures.[4-6,21] These lamellarlike hard domains have been reported by investigators of urea–urethane and urethane elastomers as being crystalline or paracrystalline in order, but they can also be amorphous.[20-23] It is also thought that upon deforming these materials the long axis of the lamellarlike domains initially orients in the stretch direction or the hard segments of these domains orient transverse to the stretch direction, which gives rise to the negative orientation.[6,21,24] Bonart and Hoffman have also suggested that for an MDI–PTMO-based urethane elastomer there exists both smaller hard segment domains (as in Fig. 1) and lamellarlike hard domains.[2] They predict that the smaller hard segment domains align in the stretch direction, giving rise to positive orientation. However, the overall negative orientation behavior that was detected at the lower elongations was attributed to the lamellarlike domains dominating the hard segment orientation behavior.[2] In comparing the hard segment orientation behavior of urethanes and urea-urethanes, one usually observes at the lower elongations more transverse orientation in the urea–urethanes.[1-6,20-22] This difference is most likely due to the stronger hydrogen bonding in the hard domains of the urea–urethanes. The stronger hydrogen bonding suggests that there is more resistance to shear stresses breaking up (disrupting) the lamellarlike domains, which, if it occurs, leads to a positive orientation result at higher elongations.

Based on the negative orientation of the hard segments in plaques 1 and 2, and the explanations given in the literature, it is speculated that the smaller hard domains and the polyurea aggregates do not necessarily possess the structures exactly portrayed in the earlier morphological model for a urethane foam proposed by Armistead et al.[11] in Figure 1, but they may or at least many may also possess a lamellarlike or rodlike texture as shown in Figure 9(a). It is possible that only one of the two types of hard domains (smaller hard segment domains or polyurea aggregate) has a lamellarlike structure as Bonart and Hoffman suggested in their model for an MDI–PTMO based urethane elastomer.[24] However, due to the significant change in the hard segment orientation behavior with deformation in both plaques 1 and 2, it does not appear that only one of these domains could be contributing to and dominating this behavior (see Figs. 6 and 7). In addition, the TEM micrographs for these plaques showed no evidence of the aggregate structure in plaque 1, but there was an indication of such structures in plaque 2.[11] Thus, it is believed that both the polyurea aggregates and the smaller hard domains possess a lamellarlike texture and are contributing to the hard segment orientation behavior as shown by the modified, but still oversimplified morphological model in Figure 9. In this model, the polyurea aggregates and the smaller domains are thought to align as a whole with their long axis in the stretch direction upon deforming the plaque. This, of course, leads to the negative hard segment orientation behavior shown in Figures 6 and 7.

As indicated earlier, a possible explanation for the difference in orientation level for the hard segments of plaque 1-DMF and 2-DMF would be provided. It appears the *local* strain on the hard segments would be greater in plaque 2 than in plaque 1 due to the lower volume content of soft segments in plaque 2. Therefore, upon deforming these materials, this greater local strain in plaque 2 suggests that more hard segment orientation would be observed for plaque 2 than for plaque 1 at the same level of elongation.

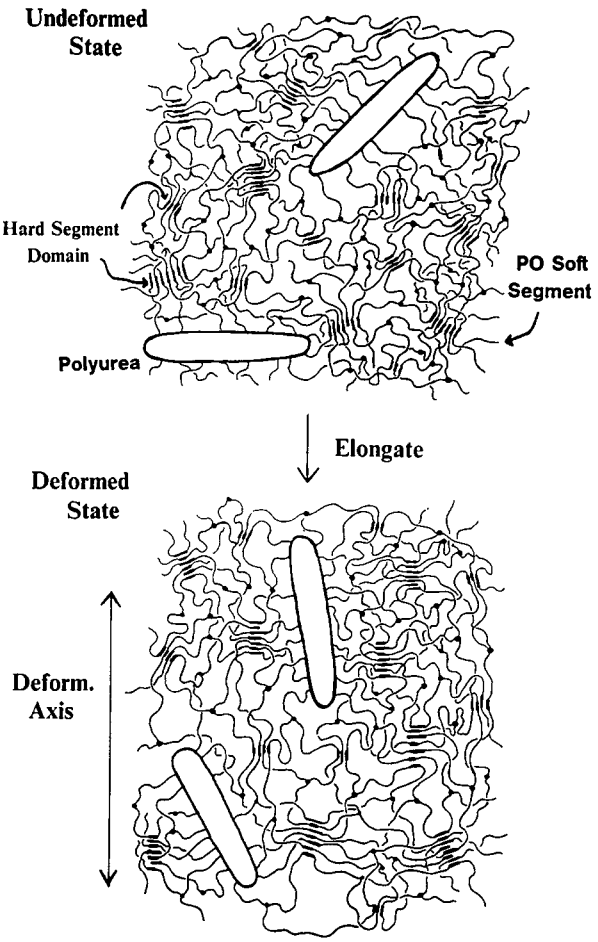

Figure 9 Modification of morphological model in undeformed (a) and deformed (b) states. Previous model shown in Figure 1. Modifications suggest that the polyurea aggregates possess a more elongated lamellar structure and that some of the hard segment domains also possess lamellarlike textures.

Lamellarlike hard segment domains are also suspected to be present in the PUU elastomer due to the two-step reaction method used to make this elastomer. The formation of these lamellarlike hard domains also appears to be driven by the symmetrical structure of its chain extender, MOCA. The structure of MOCA is similar to that of MDI in that its symmetry is thought to promote the formation of partially crystalline and paracrystalline domains in urea–urethane and urethane elastomers. The WAXS patterns of this material also show some apparent hard segment ordering, which suggests at least paracrystalline character. Thus, similarly to the plaques, the distinct transverse orientation shown in Figure 8 for the PUU elastomer is thought to be attributed to the lamellarlike hard domains orienting as a whole with their long axis aligned in stretch direction. Unlike the plaques, the PUU elastomer can be stretched to higher elongations at least partially because of its lack of a covalent network. Therefore, a positive upturn in the hard segment orientation level of the PUU elastomer is observed near elongations of 100% (see Fig. 8). This change in orientation behavior suggests some of the lamellarlike hard domains are disrupted and possibly form smaller domains. These smaller hard domains are more likely to align with the hard segment axis in the stretch direction; this event would give rise to positive orientation behavior. Other investigators of MDI-based polyurea–urethane elastomers have also suggested that positive upturn in the hard segment orientation level is due to some disruption in the lamellar hard domains.[4–6] However, the actual mechanism by which the lamellar hard domains are disrupted and the hard segments of these domains align more in the stretch direction is not fully understood and agreed upon.[4–6]

In Figure 8, the orientation function of the $\nu(C{=}O)_{ur}$ group for the PUU elastomer is below the lower limit of −0.5 defined by linear dichroism theory for uniaxial orientation. Bonart and Hoffman have also observed orientation values below −0.5 for an MDI-PTMO urea–urethane elastomer.[24] The authors in this case implied that biaxial orientation existed in the hard segments of their polymer upon deformation. It is also thought that upon deforming the PUU elastomer, the hard segments are also partially biaxially oriented. In a uniaxially deformed system, the theoretical derivation for the dichroic ratio is based on a random distribution of the chains about the stretch direction and the transition moments for $(C{=}O)_{ur}$ groups about the chains (recall Fig. 2). By considering a case of nonrandom distribution for either situation and reinspecting the derivation of the dichroic ratio, the experimental values obtained for the dichroic ratio giving orientation function values less than −0.5 have been calculated. These calculations are shown in some detail in Appendix A for the interested reader. The results of the calculations suggest that (a) the lamellarlike (lathelike) hard domains as a whole align preferably at an angle to the surface of the film and/or (b) the rigid nature or the energy barriers for free rotation of the hard segments causes the distribution of the transition moments about the chain axis to be skewed. The former is speculated to be the more probable origin of the observed biaxial orientation.

Orientation Hysteresis

The orientation hysteresis behavior with a simultaneous response was obtained by subjecting a sam-

ple to a cyclic strain test. The orientation measurements and the mechanical response were evaluated in 10% increments of strain. The cyclic stress–strain as well as the orientation behavior for plaque 2-DMF and the PUU elastomer are shown in Figures 10 and 11, respectively. The mechanical hysteresis is small for plaque 2-DMF [see Fig. 10(a)] and slightly larger for the PUU elastomer [see Fig. 11(a)]. This difference is thought to be attributed to more chain slippage or rearrangement of chains taking place in the PUU elastomer since it consists of only linear chains. On the other hand, the movement of the chains is limited in plaque 2-DMF, since it has a covalent network.

The simultaneous orientation behavior for plaque 2-DMF [Fig. 10(b)] and the PUU elastomer [Fig. 11(b)] both exhibit near reversible behavior for the hard segments, at the interface and for the soft segments (not shown). This orientation behavior is consistent with the small amount of mechanical

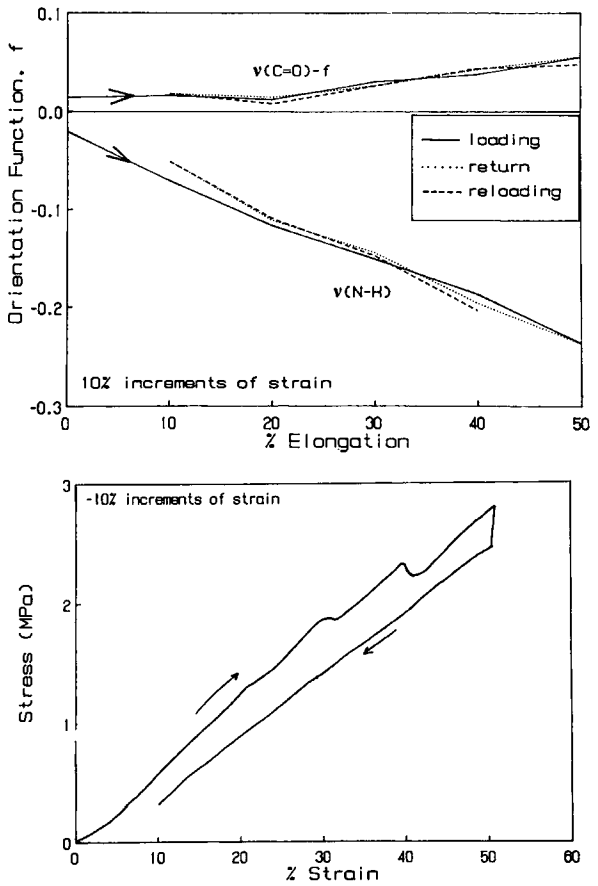

Figure 10 Mechanical (a) and orientation (b) behavior for plaque 2 during cyclic deformation. The decrease in stress during loading is due to stress relaxation in the sample.

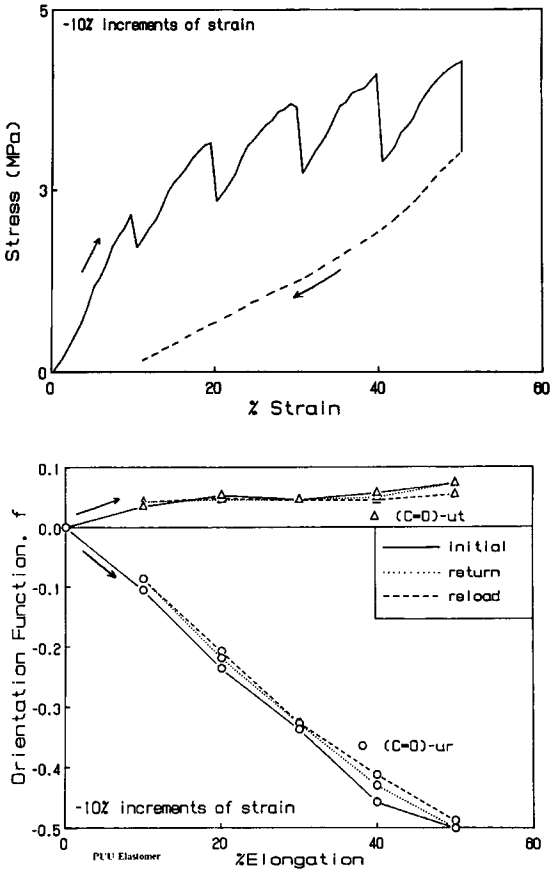

Figure 11 Mechanical (a) and orientation (b) behavior for the PUU elastomer during cyclic deformation.

hysteresis observed for both materials, as discussed above. The near reversible orientation of the hard segments suggests that the hard segment domains and the polyurea aggregates of plaque 2 as well as the lamellarlike hard domains of the PUU elastomer are not disrupted up to elongations of 50% [see Figs. 10(b) and 11(b)]. However, at initial strain levels of 125% in the PUU elastomer, significant irreversible hard segment orientation behavior is observed, while the soft segments and the interface exhibit practically reversible behavior (data not shown here). This irreversibility is attributed to some of the lamellarlike hard domains being disrupted at the higher strains, as discussed earlier. Other investigators of urea–urethane elastomers have also observed similar irreversible hard segment orientation at high strain levels and with a rather comparable explanation.[5,6] The irreversible orientation behavior of the hard segments in the PUU elastomer is also believed to be a result of an increase in the mechanical hysteresis at this higher initial elongation level of 125%.

It is possible that greater irreversible orientation behavior for the hard segments of plaque 2 (and other plaques pressed from foams) would have been obtained by stretching to higher initial elongations. However, this has not been evaluated due to sample failure of samples of plaque 2-DMF at elongations exceeding 50%.

Time-dependency Orientation

As mentioned earlier, a better understanding of the viscoelastic behavior in polyurethane foams is of importance due to its relation to compression set and fatigue. Some features of viscoelastic behavior were therefore evaluated in plaque 1 and plaque 2 as well as in the PUU elastomer after imposing a 30% strain level and then by periodically following the orientation of the different absorbing groups as well as the stress relaxation. The normalized stress relaxation response for plaque 2-DMF and the PUU elastomer are shown in Figure 12(a). For both materials, the majority of the stress relaxation takes place within the first 10 min and then begins to level off (more so in plaque 2-DMF). As one would speculate, more stress decay is observed in the PUU elastomer since it is a linear segmented system. On the other hand, the plaques possess a covalent network that allows for less rearrangement and therefore less relaxation.

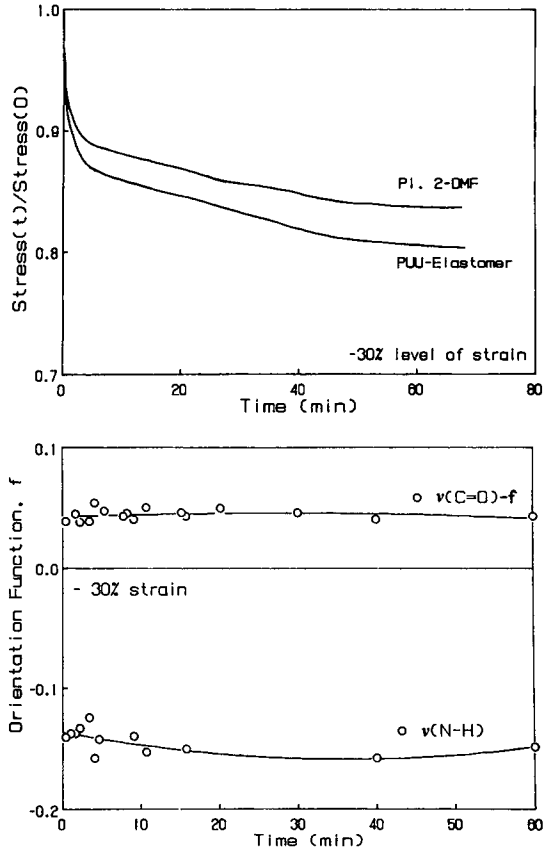

Figure 12 Normalized stress relaxation behavior (a) for plaque 2-DMF and the PUU elastomer and the orientation–time behavior (b) for plaque 2-DMF.

Even though some stress relaxation is observed for plaque 2-DMF, no significant segmental orientation changes with time are detected as shown in Figure 12(b). Similar orientation-time behavior to that of plaque 2-DMF was also obtained for plaque 1 and the PUU elastomer, and, thus, this behavior is not shown here for these two materials. Once again, the orientation-time behavior did not appear to differ in the plaques and the PUU elastomer at least at *this level* of elongation.

As shown in Figure 12(b), the changes in orientation with time at the interface and for the hard segments are not significant. This same behavior was also observed for the soft segments (not shown here). This was expected since the soft segments are known to relax quickly and most likely before the first experimental point is taken (30 s). It is also not surprising to see any significant orientation changes at the interface since the interfacial region between the hard and soft segments is thought to be influenced mostly by the soft segments. On the other hand, some significant orientation changes were anticipated to be observed in the hard segments since they are more rigid and, hence, are thought to relax slower. However, the results do not show any significant changes in orientation level with time [see Fig. 12(b)]. Therefore, the possibility exists that either the average of the orientation of the hard segments is not changing or the hard segments do reorient with time, but the changes are small and within the accuracy of the experimental measurements of the orientation function (±.05 orientation units).

CONCLUDING REMARKS

To the authors' knowledge, the segmental orientation behavior shown and discussed in this paper for the plaques thermally pressed from the foams is the first to be reported in the literature for some conventional polyurethane water-blown foams. At low strain levels (30–50%), the orientation behavior of the plaques have been shown to be similar to that of a related PUU elastomer. This observation suggests that similar forces govern the orientation changes with deformation in these materials, despite

the fact that the plaques possess a covalent network morphology while the elastomers form a linear segmented system. Furthermore, this suggestion is consistent with conclusions drawn from the morphological investigation of these foams and their respective plaques.[11]

The orientation–elongation behavior for the plaques revealed that the small hard domains as well as the polyurea aggregates likely possess a lamellarlike texture with the hard segments perpendicular to the long axis of the lamellae. This structure, which is shown schematically in Figure 9, is tentatively suggested to account for why there is negative orientation of the hard segments. The low orientation and mechanical hysteresis behavior suggests that the plaque (foam) structures do behave reversibly up to elongations of 50%. At a 30% strain level of strain, no significant segmental orientation changes with time are observed and/or detected in the plaques. In short, the work presented here has provided some additional insight of the morphology as well as some further understanding of the structure–property behavior in the solid portion of flexible polyurethane foams. Clearly, additional insight to the features of the urea aggregates and the role they play in the structure–property behavior would be desirable.

Future studies related to the work presented in this paper are necessary so that a better and more complete understanding of the important physical properties in flexible foams can be obtained. Therefore, further work is now being performed to evaluate the effect of high temperature (50–125°C) as well as exposure to humid conditions on the segmental orientation behavior and the viscoelastic response of these thermally compression-molded foams.

J. C. M. and G. L. W. would like to thank Dow Chemical for supplying the samples used in this work and for their financial support to the project.

REFERENCES

1. R. W. Seymour, A. E. Allegrezza, and S. L. Cooper, *Macromolecules,* **6,** 896 (1973).
2. R. Bonart and K. Hoffman, *Colloid Polym. Sci.,* **260,** 268 (1982).
3. H. W. Siesler, *Pure Appl. Chem.,* **57,** 1603 (1985).
4. C. B. Wang and S. L. Cooper, *Macromolecules,* **16,** 775 (1983).
5. K. Hoffman and R. Bonart, *Makromol. Chem.,* **184,** 1529 (1983).
6. I. Kimura, H. Ishihara, H. Ono, N. Yoshihara, S. Nomura, and H. Kawai, *Macromolecules,* **7,** 355 (1974).
7. C. S. P. Sung and N. S. Scheider, *Macromolecules,* **10,** 452 (1977).
8. C. S. Paik Sung, C. B. Hu, and C. S. Wu, *Macromolecules,* **13,** 111 (1980).
9. C. S. Paik Sung and C. B. Hu, *Macromolecules,* **14,** 212 (1981).
10. G. L. Wilkes and S. Abouzahr, *Macromolecules,* **14,** 458 (1981).
11. J. P. Armistead, G. L. Wilkes, and R. B. Turner, *J. Appl. Polym. Sci.,* **35,** 601 (1988).
12. R. B. Turner, H. L. Spell, and G. L. Wilkes, in *SPI 28th Annual Technical/Marketing Conference,* 1984, p. 244.
13. G. Rossmy, H. J. Kollmeier, W. Lidy, H. Schator, and M. Wiemann, *J. Cell. Plast.,* **17**(6), 319 (1981).
14. F. E. Bailey and F. E. Critchfield, *J. Cell. Plast.* **17,** 333 (1981).
15. G. Hauptman, K. H. Dorner, J. Hocker, and G. Pfister, in *Cellular and Non-cellular Polyurethanes,* International Conference, Strassbourg, France, Urethane Division, SPI, 1980.
16. J. P. Armistead, Master Thesis, Virginia Polytechnic Institute and State University, Blacksburg, VA, 1985.
17. R. D. B. Fraser, *J. Chem. Phys.,* **21,** 1511 (1953).
18. J. L. White, *J. Polym. Eng.,* **5,** 277 (1985).
19. R. S. Stein, personal communication.
20. V. A. Khranovskii and L. P. Gul'ko, *J. Macromol. Sci. Phys.,* **B22**(4), 497 (1983).
21. I. Ishihara, I. Kimura, K. Saito, and H. Ono, *Macromol. Sci. Phys.,* **B10**(4), 591 (1974).
22. R. Bonart, L. Morbitzer, and G. Hentze, *J. Macromol. Sci.,* **B3,** 337 (1969).
23. R. Bonart, *J. Macromol. Sci. Phys.,* **B2**(1), 115 (1968).
24. K. Hoffman and R. Bonart, *Colloid Polym. Sci.,* **262,** 1 (1984).

APPENDIX A: POSSIBLE EXPLANATION FOR BIAXIAL ORIENTATION

Problem

Some of the orientation values for $(C{=}O)_{ur}$ groups were less than −0.5 (lower limit for uniaxial orientation). The lowest value was −0.6, which corresponds to a dichroic ratio, D, equal to 2.35 ($\alpha = 90°$).

Approach

The dichroic ratio is determined by evaluating the experimental values of $A_{\|}$ and $A_{\perp}$ and then taking the ratio of $A_{\|}$ to $A_{\perp}$. Thus, in determining why the dichroic ratio is greater than 2 or the orientation function is less than −0.5, the derivation of D given by Fraser will be examined.[17] The following two cases will be considered separately:

1. The chains (hard segments) are unsymmetrically distributed about the stretch direction.

2. The transition moment of the $(C{=}O)_{ur}$ groups are *unsymmetrically* distributed about the chain axis.

The absorbance, A, of a given chromophoric group is defined as

$$A \propto (\mathbf{P} \cdot \mu)^2 \qquad \text{(A.1)}$$

where $\mathbf{P}$ is the electric vector of the polarized and μ is the transition moment vector of the chromorphoric group. From the coordinate system shown in Figure A.1, the following relationships can now be derived for this case—a) parallel polarized radiation:

$$(\mathbf{P}_{\parallel} \cdot \mu)^2 = \cos^2\alpha \cos^2\beta + \sin^2\alpha \sin^2\psi \sin^2\beta \qquad \text{(A.2)}$$

(b) perpendicular polarized radiation:

$$(\mathbf{P}_{\perp} \cdot \mu)^2 = \cos^2\alpha \sin^2\beta \sin^2\phi + \sin^2\alpha \cos^2\psi \cos^2\phi + \sin^2\alpha \sin^2\psi \cos^2\beta \sin^2\phi \qquad \text{(A.3)}$$

The dichroic ratio for a given absorption band is defined as average of the expression in eq. (A.2) divided by the average of the expression in eq. (A.3).

For *case 1*, if the assumption is made that the chains lie at one angle, ϕ, and all possible orientations over ψ are probable, then

$$D = \frac{\frac{1}{2\pi}\int_0^{\pi} |\mathbf{P}_{\parallel} \cdot \mu|^2 \, d\psi}{\frac{1}{2\pi}\int_0^{\pi} |\mathbf{P}_{\perp} \cdot \mu|^2 \, d\psi} \qquad \text{(A.4)}$$

and substituting in eqs. (A.2) and (A.3) into eq. (A.4) and letting α and β equal 90°, D becomes

$$D = \frac{1}{\cos^2\phi} \quad \phi = \cos^{-1}\left(\frac{1}{D}\right)^{0.5} \qquad \text{(A.5)}$$

Thus, for $D = 2.35 \rightarrow \phi \geq 49.3°$.

For *case 2*, if the assumption is made that the transition moments for $(C{=}O)_{ur}$ lie at an angle ψ and all possible orientations over ϕ are probable, then

$$D = \frac{\frac{1}{2\pi}\int_0^{\pi} |\mathbf{P}_{\parallel} \cdot \mu|^2 \, d\phi}{\frac{1}{2\pi}\int_0^{\pi} |\mathbf{P}_{\perp} \cdot \mu|^2 \, d\phi} \qquad \text{(A.6)}$$

and substituting in eqs. (A.2) and (A.3) into eq. (A.6), and again letting α and β equal 90°, D becomes

$$D = 2\tan^2\psi \quad \psi = \tan^{-1}\left(\frac{D}{2}\right)^{0.5} \qquad \text{(A.7)}$$

Thus, for $D = 2.35 \rightarrow \psi \geq 47.3°$.

For the two cases (ϕ, ψ), for D equal to 2.35, the azimuthal angle for which the chains are oriented is equal to 49.3° and that of the transition moments is equal to 47.3°. The case for which the hard segments align at an angle approximately 49° or the distribution of chains are preferentially aligned at or near to the film surface, is possible since these hard segments are part of lamellarlike domains. In other words, the lamellarlike domains as a whole could be aligning at an angle to the surface as well as transverse to the stretch direction. In the second case, steric hindrance of the hard segments could cause the transition moment of $(C{=}O)_{ur}$ to be aligned at an angle about the chain axes or to have a nonrandom distribution such that the angle about the chain axes is heavily weighted toward 47°.

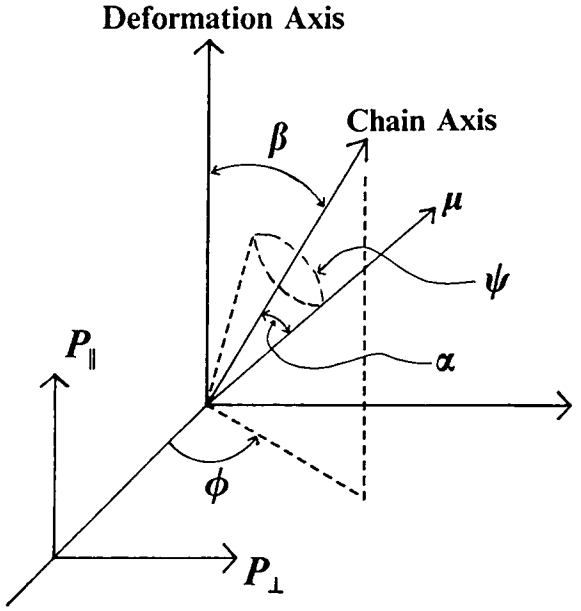

Figure A.1 Coordinate system for derivation of dichroic ratio (ψ and ϕ represent the azimuthal dependence of an absorbing group about its chain axis and the chain axis about the deformation axis, respectively).

Received January 15, 1990
Accepted December 3, 1990